International Journal of Science and Research (IJSR)
ISSN: 2319-7064
ResearchGate Impact Factor (2018): 0.28 | SJIF (2018): 7.426

Modeling and Simulation of Hybrid Wind and Photovoltaic Stand-Alone Generation System

Vishal Sharma

M.Tech.(Power System)-IV Semester Student 2018-2019, Career Point University, Kota, Rajasthan, India

Abstract: ***This work focuses on the modelling and analysis of a Standalone wind-PV Hybrid generation system under different conditions in MATLAB/SIMULINK environment. The proposed system consists of two renewable sources i.e. wind and solar energy. Modelling of PV array and wind turbine is clearly explained. It works as an uninterruptible power source that is able to feed a certain minimum amount of power into the load under all conditions. Power transfer was different modes of operation, including normal operation without use of battery, which gives the user-friendly operation. A control strategy regulates power generation of the individual components so as to give the hybrid system to operate in the proposed modes of operation. These two systems are combined to operate in parallel and the common DC bus collects the total energy from the wind and photovoltaic subsystems and uses it partly to charge the battery and partly to the DC load. This paper offers a useful wind-PV hybrid model which can be used for performance analysis of such systems.***

1. Introduction

The rising consumption rate of fossil fuels and the pollution problem associated with them has drawn worldwide attention towards renewable energy sources. With increasing load demand and global warming, many are looking at environment friendly type of energy solutions to preserve the earth for the future generations. Other than hydro power, many such energy sources like wind and photovoltaic energy holds the most potential to meet our energy demands. While some others like fuel cells are in their advanced developmental stage. These generation systems have been attracted greatly all over the world. The integration of renewable energy sources and energy-storage systems has been one of the new trends in power-electronic technology. The world's fastest growing energy resources, a clean and effective modern technology that provides a hope for a future based on sustainable, pollution free technology. The increasing number of renewable energy sources requires new strategies for their operations in order to maintain or improve the power-supply stability, quality and reliability. Today's photovoltaic and wind turbines are state-of-the-art of modern technology-modular and very quick to install. A combination of two or more renewable energy sources is more effective as compared to single source system in terms of cost, efficiency and reliability. The common types of AC generator in modern wind turbine systems are as follows: Squirrel-Cage rotor Induction Generator; However, in this paper the variable-speed directly-driven multi-pole permanent magnet synchronous generator (PMSG) wind architecture is chosen for this purpose, it offers better performance due to higher efficiency and less maintenance because it does not have rotor current. Wound-Rotor Induction Generator; Doubly-Fed Induction Generator; Synchronous Generator (With external field excitation); and Permanent Magnet Synchronous Generator [3]. PMSG can be used without a gearbox, which implies a reduction of the weight of the nacelle and reduction of costs [3].Standalone Wind/PV hybrid generation system offers a feasible solution to distributed power generation for isolated localities where utility grids are not available. It is also free from pollution what makes it more attractive. For isolated localities, one practical approach to self-sufficient power generation involves using a wind turbine and PV system with battery storage to create a stand-alone hybrid system [3, 4]. A photovoltaic (PV) system is the most simple and reliable way to produce electricity from the conversion of solar energy. The basic building device of SPV system is SPV cell. The output of SPV system may be directly fed to the loads or may use a power electronic converter to operate it at its maximum power point. [7,8]. Each of the two subsystems; namely PV subsystem and wind subsystem is controlled by its own controller. Each controller will guide its own system to track the maximum power [6, 7]. The aim of this paper is to provide the reader with all necessary information to develop wind turbine models and PV panel that can be used in the simulation for a standalone wind/PV generation system and for further study of such systems. This paper includes in details the equations that form the wind turbine and PV panel. The two systems are combined to operate in parallel. The main task of this paper is to develop a simulation model of a standalone hybrid generation System including wind and PV subsystems using MATLAB/ SIMULINK system. Characteristics of modelled wind turbine and PV panel have been shown for different conditions.

2. Proposed Hybrid Energy System

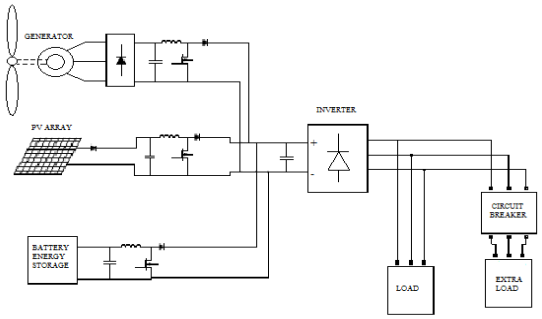

Figure 1: Configuration of Hybrid Energy System

A. Wind Energy Source The wind turbine captures the wind's kinetic energy in a rotor consisting of two or more blades mechanically coupled to an electrical generator. The

Licensed Under Creative Commons Attribution CC BY

equation describes the mechanical power captured from wind by a wind turbine can be formulated as:

$$P_m = 0.5\rho A C_p V^3 \quad (1)$$

Where:
ρ = Air density (Kg/m3)
A = Swept area (m2)
C_p = Power coefficient of the wind turbine
V = Wind speed (m/s)
t = Time (sec)

The pitch angle refers to the angle in which the turbine blades are aligned with respect to its longitudinal axis. The theoretical maximum value of the power coefficient C_p is 0.59. It is dependent on two variables, the tip speed ratio (TSR) and the pitch angle. *TSR* is defined as the linear speed of the rotor to the wind speed.

$$TSR = \lambda = \frac{\omega R}{V} \quad (2)$$

Where:
ω=Turbine rotor speed (rad/s)
R= Radius of the turbine blade (m)
v = Wind speed (m/s)

The amount of aerodynamic torque Tw in N-m is given by the ratio between the power extracted from the wind and the turbine rotor speed ww in rad/s, as follows

Tw = Pw/ Ww

Mechanical torque transmitted to the generator is the same as the aerodynamic torque since there is no gearbox. The power coefficient Cp reaches maximum value equal to 0.593 which means that the power extracted from the wind is always less than 59.3% (Betz's limit) because various aerodynamic losses depend on rotor construction [8, 9].

Fig.2 shows a typical "C_p Vs. λ" curve for a wind turbine. In practical designs, the maximum achievable C_p ranges from 0.4 to 0.5 for high speed turbines and 0.2 to 0.4 for slow speed turbines. Fig.2 shows that C_p has its maximum value(C_{pmax}) at λopt. Which results in optimum efficiency and maximum power is captured from wind by the turbine. Fig. 3 clarifies the output power of a wind turbine versus rotor speed while wind speed is changed from v1 to v4 (v4>v3>v2>v1). Fig. 3 shows that if speed is v1, at rotor speed ω1 maximum power could be captured. While speed increases from v1 to v4, similar to the maximum power point tracking rotor speed is also increases from ω1 to ω4.

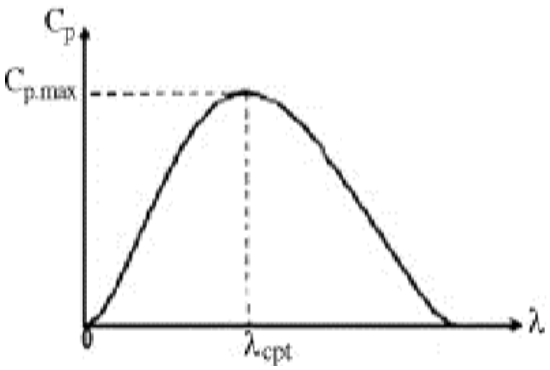

Figure 2: Power coefficient Vs Tip Speed Ratio

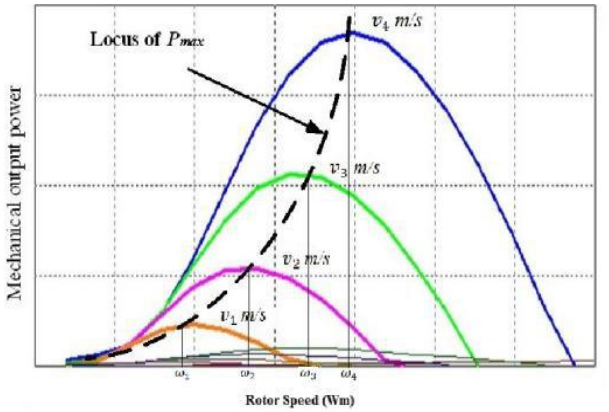

Figure 3: Output Power Vs Rotor Speed of different speeds

B. Photovoltaic (PV) System

A solar cell is the most fundamental component of a photovoltaic (PV) system. The PV array is constructed by many series or parallel connected solar cells to obtain required current, voltage and high power [10]. The equivalent circuit of a solar cell is the current source in parallel with a diode of a forward bias. Each Solar cell is similar to a diode with a p-n junction formed by semiconductor material. It can be seen that a maximum power point exists on each output power characteristic curve. The Fig: 5 shows the (I-V) and (P-V) characteristics of the PV array at different solar intensities. When the junction absorbs light, it can produce currents by the photovoltaic effect. The output power characteristic curves for the PV array at an in solution are shown in Fig. 4. The output terminals of the circuit are connected to the load. The current equation of the solar cell is given by:

$$I = I_{ph} - I_D - I_{sh} \quad (3)$$

$$I = I_{ph} - I_0\left[exp\left(\frac{qV_D}{nkT}\right)\right] - \frac{V_D}{R_{SH}} \quad (4)$$

Where: I_{ph} = Photo current (A)
ID = Diode current (A)
I_{SH} = Shunt current (A)
VD = Voltage across diode (Volt)
I_0 = Diode reverse saturation current (A)
q = Electron charge = 1.6X10-19 (C)
k = Boltzman constant = 1.38X10-23 (J/K)
T = Cell temperature (K)
Rs = series resistance (Ω)
R_{SH} = shunt resistance (Ω)

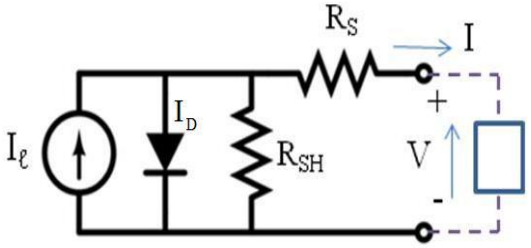

Figure 4: Equivalent circuit of PV Module

The power output of a solar cell is given by

$$P_{PV} = V * I \quad (5)$$

Where: I = solar cell output current (A)
V = Operating voltage of solar cell (volt)
P_{PV} =Output power of solar cell (W)

Licensed Under Creative Commons Attribution CC BY

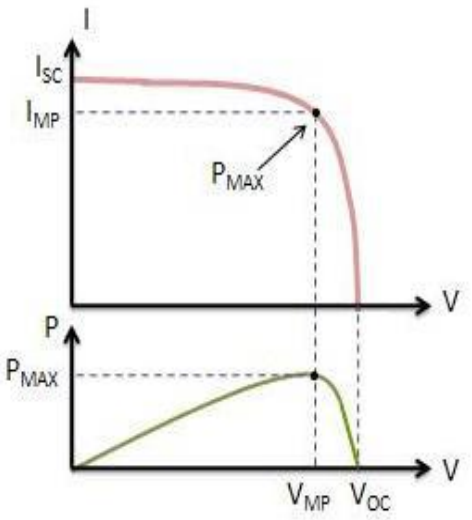

Figure 5: Output characteristics of PV Array

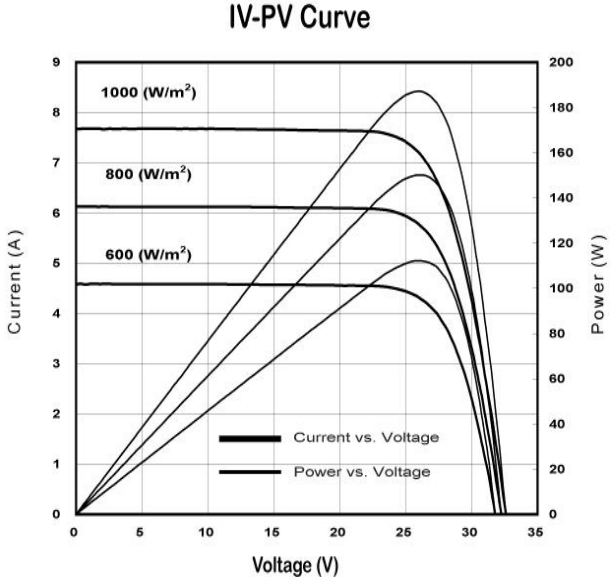

Figure 6: I-V and P-V Characteristics of PV Array at different solar intensities

C. Battery Energy Storage: Battery energy storage system (BESS) are includes batteries, control system and power electronic devices for conversion between alternating and direct current. Different types of batteries have various advantages and disadvantages in terms of power and energy capabilities, size, weight, and cost. The main types of battery energy storage technologies are: Lead-Acid, Nickel Cadmium, Sodium Sulfur, Nickel Metal Hydride and Lithium-Ion. Lead-Acid batteries, achieve high discharge rates by using deep-cycle batteries. Overall, with low maintenance requirements, relatively low self-discharge rates, Lead-Acid batteries offer a competitive solution for energy storage applications. The batteries convert electrical energy into chemical energy for storage. Batteries are charged and discharged using DC power, regulates the flow of power between batteries and the energy systems is done by a bi-directional power electronic devices. Sodium Sulfur batteries have high energy density, high efficiency of charge/discharge and long cycle life. Low energy density, non-environment friendly electrolyte and a relatively limited life-cycle are the limiting factors to its dominant use in urban renewable energy systems [16]. Nickel Cadmium (NiCd) batteries achieve higher energy density, longer cycle life and low maintenance requirements than the Lead-Acid batteries. But, which include the toxic-heaviness of cadmium and higher self-discharge rates than Lead-Acid batteries. Also, NiCd batteries may cost up to ten times more than a Lead-Acid battery [17], making it a very costly alternative. Nickel Metal Hydride (NiMH) is compact batteries and provides lightweight used in hybrid electric vehicles and tele-communication applications. According to [18], NiMH batteries can substitute NiCd batteries in communications. They also provide equivalent cycle life characteristics, are environmentally friendly and can provide for an additional capacity ranging from 25 to 40% [18]. They are currently used in cellular phones, computers, etc. and development of this technology is used in distributed energy storage applications. But, high cost [19] and limited applications of technology. With the high rate of progress in development of lithium-ion technology, it has dominated the electronics market. Lithium-Ion technology has the highest energy density amongst all types of batteries [19]. Because of the sizes it is used in small, medium and large scale renewable energy systems. During coupled operation, Changes in the wind and solar PV generation output will cause an immediate change in the BESS output and BESS must neutralize by quick changes in output power. Rate variation control (or ramp rate control) and it is applied for smoothing real power fluctuations from an associated coupled system. The information is processed by the Battery Energy System controller estimates the state of charge (SOC) of each battery cell and capacity of each battery cell, and protects all the cells operate in the designed SOC range. The amount of electrochemical energy left in a battery is measured by SOC. Allowable ramp rates are typically specified by the utility in kilowatts per minute (kW/min), and are a common feature of wind and solar power purchase agreements between utilities and independent power producers. SOC is mainly because of differences in chemical and electrical characteristics from manufacturing, aging, and ambient temperatures. When this SOC is left without any control, such as cell equalization, the energy storage capacity decreases severely. The SOC information is then used to control the charge- equalization. It is expressed as a percentage of the battery capacity. The electrochemical reaction inside batteries is very complicated and hard to model electrically in a reasonably accurate way. SOC is explained in [12] [13]. Thus, charge equalization is necessary to minimize the mismatches across the battery and extend the battery life cycle. Generally, SOC is maintained between 30%-70% to get the longer life cycle for the battery.

3. Maximum Power Point Tracking

Maximum power point tracking technique is used to improve the efficiency of both the solar panel and wind turbine and they adjusted to operate at their point of maximum power. There are different techniques for maximum power point tracking (MPPT) methods have been developed and implemented. The corresponding output powers of the two systems are measured. If this power does not correspond to their maximum powers, then their initial reference values are incremented or decremented by one step. Few of the most popular techniques are: Perturb and Observe (hill climbing method), Incremental Conductance method, Fractional short circuit current, Fractional open circuit voltage, Neural networks, Fuzzy logic. The above steps are repeated till the

Licensed Under Creative Commons Attribution CC BY

maximum power points of the wind turbine and photovoltaic array are reached. Fig. 5 shows the characteristic power curve for a PV array. The MPPT Technique depends on the initial reference rotor speed for the wind turbine and an initial reference voltage for the photovoltaic array. If this adjustment leads to an increase in their output powers then the next adjustment is made in the same direction and vice-versa. The problem considered by MPPT techniques is to automatically find the voltage *VMP* or current *IMP* at which a PV array should operate to obtain the maximum power output *PMAX* under a given temperature and irradiance.

4. Wind-PV Hybrid Generation System

Figure 7 shows the proposed system which consists of a wind turbine, a variable speed direct-drive wind generator, a wind side ac/dc converter, a solar array, dc/dc converters and a common dc load in parallel with a battery. Mechanical energy from the wind turbine drives the wind generator to generate a.c. electric power, which is converted into d.c. power to form the common dc link. PV array generates dc power [6, 7]. Each of the two subsystems; namely PV subsystem and wind subsystem is controlled by its own controller. Each controller will guide its own system to track the maximum power [6, 7, 18].The system power output depends on the climatic conditions (wind, sun), and on the battery state of charge. It can be tested for different system operations.

The control strategy used here controls the battery state of charge by keeping the DC bus voltage around the rated battery voltage (i.e.48V).The wind subsystem is a 480 W wind generator equipped of a direct driven permanent-magnet synchronous generator (PMSG), a diode rectifier and a (DC/DC) buck converter for the tracking of the maximum power point.

A 420 W photovoltaic panel is used, whose variable DC output voltage is controlled by another (DC/DC) buck used for the MPPT. The common DC bus collects the total energy from the wind and photovoltaic subsystems and uses it partly to charge the battery and partly to the DC load. Figure 7 shows the block diagram of simulated standalone hybrid PV-Wind system.

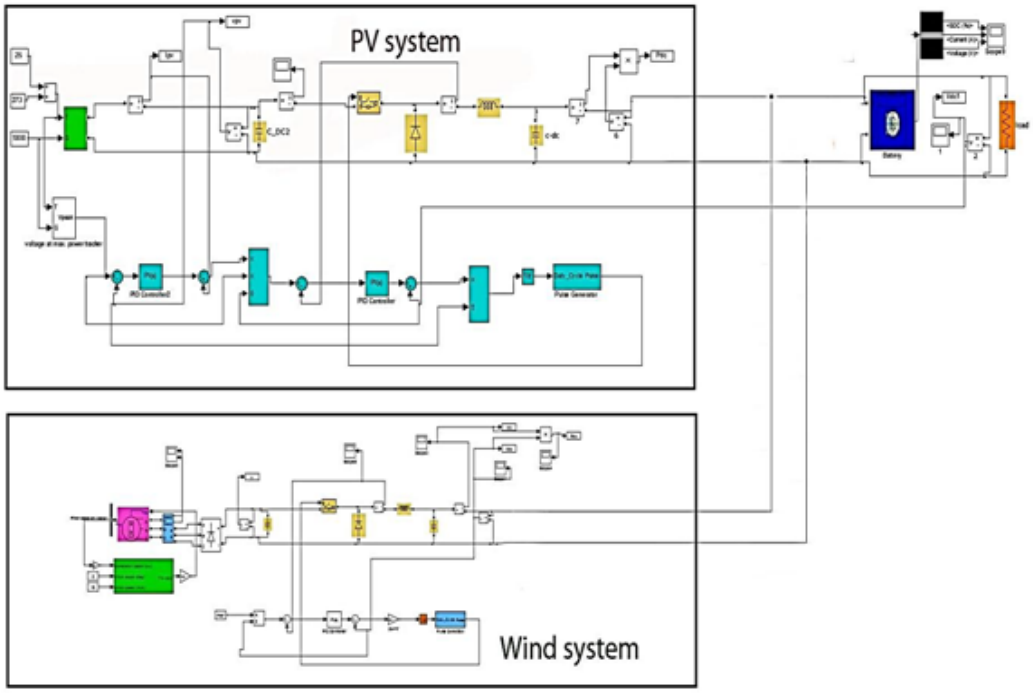

Figure 7: Block diagram of standalone hybrid system

5. Simulation Results

Simulation results of PV module

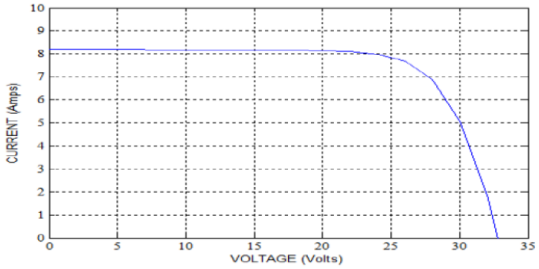

Figure 8: V-I curve of PV module

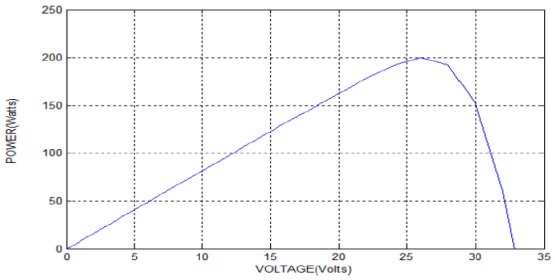

Figure 9: P-V curve of PV module

Fig 8, 9 represent the I-V and P-V characteristics of a PV module. From fig 8 we can see that short circuit current (Isc) of PV module is approximately 8.5A and open circuit voltage (Voc) is approximately 33.2 volts. From fig 9 we can

Licensed Under Creative Commons Attribution CC BY

observe that maximum power is approximately 210W and it occurs at a current of 7.69A and voltage at 26.8V approximately.

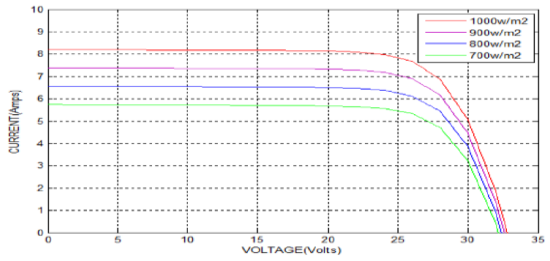

Figure 10: Effect of variation of irradiation on I-V characteristics

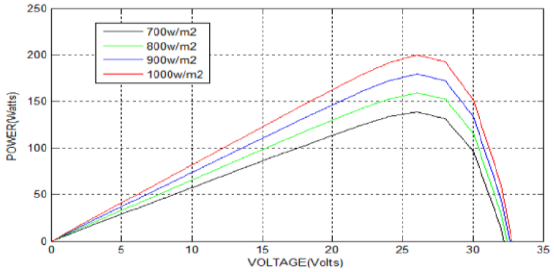

Figure 11: Effect of variation of irradiation on P-V characteristics

In fig 10, 11 we can see the effect of change in solar irradiation on PV characteristics. Fig 11 shows the effect of variation of solar irradiation on P-V characteristics. As solar irradiation increases, power generated also increases. Increase in power is mainly due to increment in current. From fig 10 we observe that as we increase the solar irradiation short circuit current increases. Variation in Solar irradiation effects mostly on current, as we can observe from fig 10 as we increase solar irradiation from 750 w/m2 to 1050 w/m2 current increases from 5.7A to 8.2A approximately but effect of variation of solar irradiation on voltage is very less.

Effect of variation of temperature

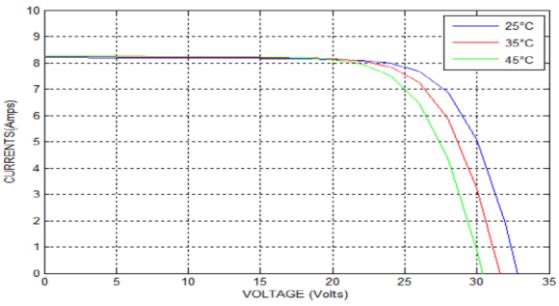

Figure 12: Effect of variation of temperature on I-V characteristics

As temperature increases power generated decreases, because on increment of temperature voltage decreases. The outcome of variation of temperature on I-V characteristics is shown in the fig 12. From the fig 12 we can see the variation of temperature mostly effects voltage, as we increase the temperature voltage decreases but current remains almost unaltered. Fig 13 shows effect of temperature variation on the P-V characteristics.

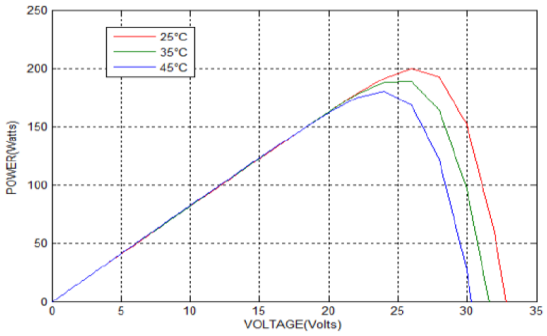

Figure 13: Effect of variation of temperature on P-V characteristics

Shading effect on PV array

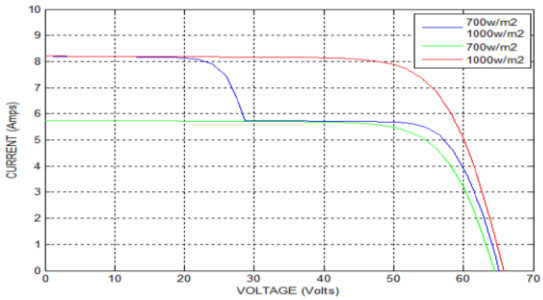

Figure 14: V-I characteristics in partial shading condition

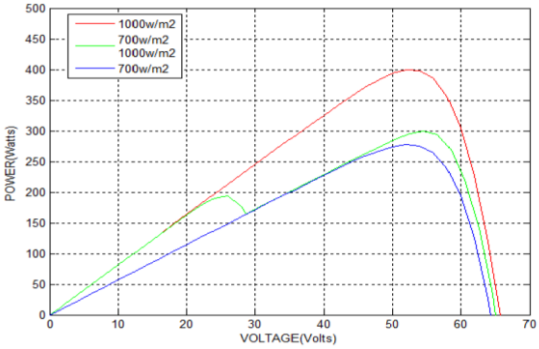

Figure 15: P-V characteristics in partial shading condition

Under partially shading condition we can observe more than one maximum power picks from fig 15. I-V, P-V characteristics of a PV array in shading condition can be seen in fig. 14 and fig 15. As we can observe from fig 15 partially shaded PV modules generate less current than the unshaded module.

Outputs after MPPT

Output power and output voltage after maximum power point tracing are manifested in the figures 16 and 17 respectively. From fig 16 we can see the maximum power which is approximately 210 watts can be tracked. As we observe from the fig 9, maximum power is achieved at voltage 26.7 volts; from fig 17 we can see we are able to track the output voltage where we can get the maximum power which is approximately 26.7 volts.

Licensed Under Creative Commons Attribution CC BY

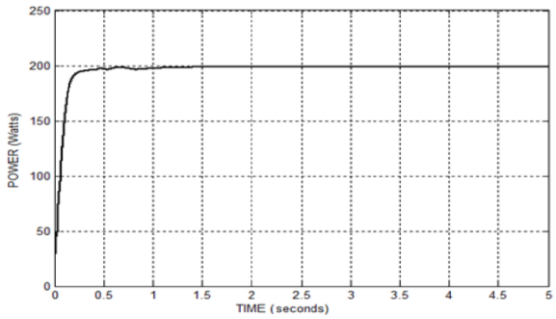

Figure 16: Output power of PV module after MPPT

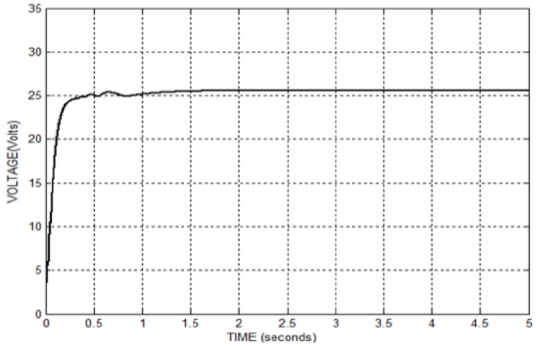

Figure 17: Output voltage of PV module after MPPT

Simulation result of wind energy system

Fig 18 shows turbine power characteristics at different wind speed. From the fig 18 we can observe that as wind speed increases turbine output power also increases.

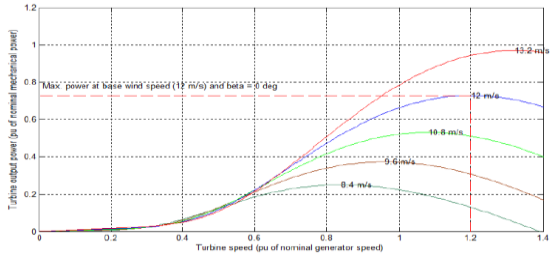

Figure 18: Turbine Power characteristics (pitch angle beta=0°)

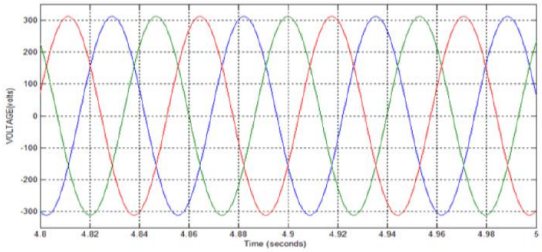

Figure 19: Three phase line output voltage of PMSG

Output Voltage of wind generator at which maximum power is achieved is shown in the fig 21. PMSG output is shown in the fig 19.The point of operation of crest power of wind generator output is traced by a maximum power point tracing system is shown in the fig 20 given below.

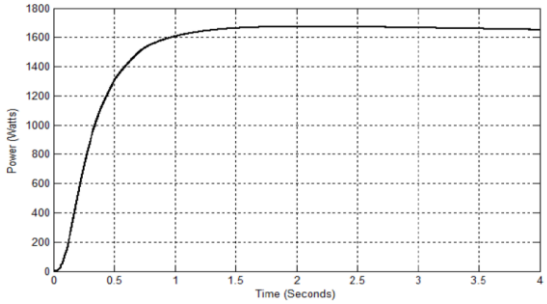

Figure 20: Output power of wind system after MPPT

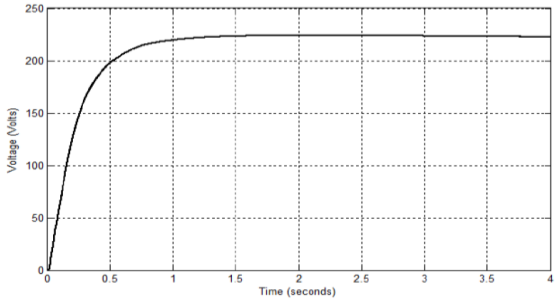

Figure 21: Output voltage of wind system at MPP

Simulation results of charging/ discharging

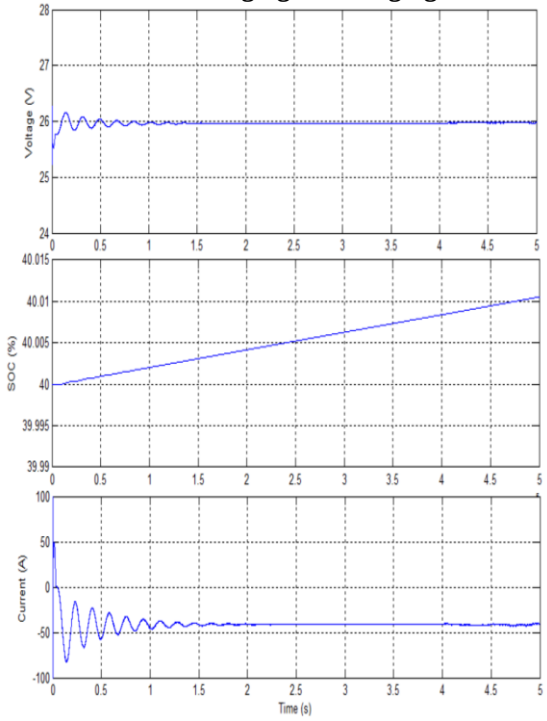

Figure 22: Charging characteristics of battery

We can observe at 42% SOC battery voltage is around 28 volts, as state of charge of battery is increased battery voltage exceeded its nominal voltage. From fig 22 we can observe that during charging state of charge (SOC) of the battery is gradually increasing and also during charging current is negative.

Licensed Under Creative Commons Attribution CC BY

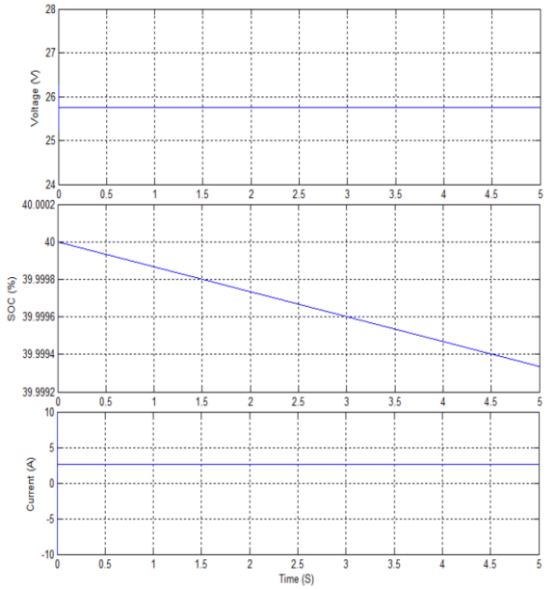

Figure 23: Discharging characteristics of battery

From fig 23 we can see during discharging, battery start supplying constant voltage and state of charge start decreasing and also during discharging current become positive, which shows battery is supplying the power to the load. Fig:24 simulation output is followed by table:1, 2, 3 on MATLAB software[1,2].

Table 1: Result of PV System

G	Load	PV		
W/m2	KW	I(A)	V(V)	P(W)
1050	32	69.20	761.8	5.29e+04
550	32	33.65	735.6	2.51e+04
265	32	15.99	715.7	1.17e+04
0	32	0	705.4	0
1050	42	69.19	750.6	6.03e+04
550	42	33.59	716.7	2,46e+04
265	42	15.99	705.4	1.15e+04
0	42	0	691.1	0

Table 2: Result of Wind System

G	Load	Wind		
W/m2	KW	I(A)	V(V)	P(W)
1050	32	8.76	615.98	5274.88
550	32	9.11	615.33	5584.90
265	32	7.23	614.88	4382.05
0	32	2,65	614.40	1580.86
1050	42	19.33	615.68	8500
550	42	10.21	614.85	6254.98
265	42	5.59	614.29	3399.06
0	42	0.66	613.69	344.12

Table 3: Result of battery System

G	Load	Battery	(I & P)
W/m2	KW	I(A)	P(W)
1050	32	12	7618
550	32	-6	-3678
265	32	-17	-1.09e+04
0	32	-27	-1.82e+04
1050	42	12	7512
550	42	-17	-1.15e+04
265	42	-27	-1.89e+04
0	42	-27	-1.78e+04

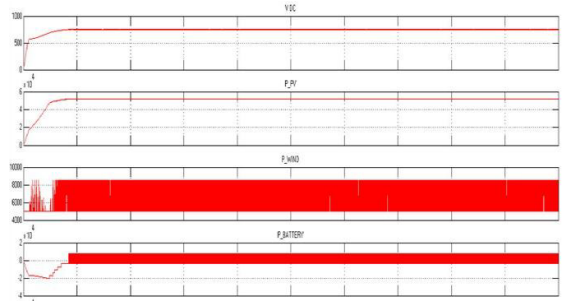

Figure 24: Power at insolation 1050 w/m2, load 42 KW

6. Experimental Study

The system under the condition where the wind source has failed and only the PV source is supplying power to the load. Finally the simultaneous operation of the two sources when sudden load is occurred. Sometimes sudden load causes fluctuations. However, this fluctuation must be suppressed. One existing method to solve these issues is to install batteries which absorb power from the system as shown in Fig. 1. Using this method the PV/WT hybrid generation system can supply almost good quality power are power supplied by the battery. However, this method has disadvantages that they require batteries which are costly. Moreover, they cannot guarantee certainty of load demands at all times especially at bad environmental conditions, where there is no power from the PV and Wind generation system. A 10kW of the load connected hybrid system was developed. Additional load of 4kW is connected by using a circuit breaker in a specified time. Fig. 1 shows the System. It is composed of a PV converter, a wind converter, a BESS converter, and a grid inverter.

7. Conclusion

In this paper a multi-input energy system for hybrid wind/solar energy systems have been presented. ASIMULINK model of the Wind-PV hybrid generation system is proposed and all the necessary models of the system components were addressed. Either wind or solar system is supported by the battery to meet the load. Also, simultaneous operation of wind and solar system is supported by battery for the same load. Dynamic modelling and simulations of the hybrid system is proposed using SIMULINK. Various results were obtained at different operating conditions and these results were found to be satisfactory. Load demand is met from the combination of PV array, wind turbine and the battery. Various results were obtained at different operating conditions and these results were found to be satisfactory. Power sharing by each subsystem was also found to be in accordance. This paper is very useful for modelling and for basic analysis of Wind-PV hybrid system. With further modification this model can be used for the modelling of Grid connected Wind-PV system.

8. Acknowledgement

The Author Vishal Sharma gratefully acknowledges the guidance and encouragement provided by Mr. Ravindra Meena, Assistant Professor, Career Point University, Kota, Rajasthan.

Licensed Under Creative Commons Attribution CC BY

References

[1] M.MAHALAKSHMI, Dr. S. LATHA," modeling, simulations and sizing of photovoltaic/wind/fuel cell hybrid generation system" International Journal of Engineering Science and Technology (IJEST), Vol. 4 No.05 May 2012.
[2] M.M Hoque , I.K.A Bhuiyan , Rajib Ahmed, A.A. Farooque & S.K Aditya," Design, Analysis and Performance Study of a Hybrid PV Diesel - Wind System for a Village Gopal Nagar in Comilla", Global Journal of Science Frontier Research Physics and Space Sciences Volume 12 Issue 5 Version 1.0 year 2012.
[3] Alejandro Rolan, Alvaro Luna, Gerardo Vazquez, Daniel Aguilar, Gustavo Azevedo, " Modeling of a Variable Speed Wind Turbine with a Permanent Magnet Synchronous Generator ". IEEE International Symposium on Industrial Electronics (ISlE 2009) Seoul Olympic Parktel, Seoul, Korea July 5-8, 2009.
[4] Polinder H., de Haan S. W. H., Dubois M. R., Slootweg J., "Basic Operation Principles and Electrical Conversion Systems of Wind Turbines", NORPIE / 2004, Nordic Workshop on Power and Industrial Electronics, Paper 069, Trondheim, Norway, 14-16 June, 2004.
[5] MittalR., Sandhu K. S.and Jain D. K. "Low voltage ride-through (LVRT) of grid interfaced wind driven PMSG," ARPN Journal of Engineering and Applied Sciences., 2009, vol. 4, no. 5. Pp. 73-83.
[6] Dali M., Belhadj, J., Roboam, X. and Blaquiere, J.M. "Control and energy management of a wind photovoltaic hybrid system", Proc. EPE Conference, 2-5 Sept. 2007, pp 1-10.
[7] Dali M., Belhadj J., Roboam X., "Hybrid solar-wind system with battery storage operating in grid–connected and standalone mode: Control and energy management - Experimental investigation", Energy 35 (2010) 2587-2595.
[8] Akhmatov V., "Variable-Speed Wind Turbines with Doubly-Fed Induction Generators Part III: Model with the Back-to-back Converters", Wind Engineering, Volume 27, No. 2, pp 79-91, 2003
[9] Hansen A.D., Michalke G., "Modelling and control of variable speed multipole PMSG wind turbine", submitted to Wind Energy, 2007.
[10] Hong-Woo Kima, Sung-SooKimb, Hee-Sang Koa, "Modeling and control of PMSG-based variable-speed wind turbine", Electric Power Systems Research 80 (2010) 46–52.
[11] I. Altas, A.M.Sharaf, 2007 "A photovoltaic array (PVA) simulation model to use in Matlab Simulink GUI environment." IEEE I-4244- 0632 -03/07.
[12] Marcelo GradellaVillalva, Jonas Rafael Gazoli, Ernesto RuppertFilho, "Modeling and circuit-based simulation of photovoltaic arrays", 10th Brazilian Power Electronics Conference (COBEP), 2009.
[13] J. Hyvarinen and J. Karila.New analysis method for crystalline silicon cells.In*Proc. 3rd World Conferenceon Photovoltaic Energy Conversion*, v. 2, p. 1521–1524, 2003.
[14] E. Koutroulis, K. Kalaitzakis, and V. Tzitzilonis. Development of a FPGA-based system for real-time simulation of photovoltaic modules. *Microelectronics Journal*, 2008.
[15] Geoff Walker. Evaluating MPPT converter topologies using a matlab PV model.*Journal of Electrical & Electronics Engineering, Australia*, 21(1), 2001.
[16] W. De Soto, S. A. Klein, and W. A. Beckman. Improvement and validation of a model for photovoltaic array performance.*Solar Energy*, 80(1):78–88, January 2006.
[17] Glass.M.C., "Improved solar array power point model with SPICE realization," in *Proc. 31st Intersoc. Energy Convers.Eng.Conf. (IECEC),* 1996, vol. 1, pp. 286–291.
[18] Kuo.Y.C., Liang.T.J. andChen.J.F., "Novel maximum-power-point tracking controller for photovoltaic energy conversion system," *IEEE Trans. Ind. Electron.*, 2001, vol. 48, no. 3, pp. 594– 601.Conclusion

Licensed Under Creative Commons Attribution CC BY